

section, as might be expected when the photon wavelength is smaller than the pion Compton wavelength.²⁹

One of our original reasons for undertaking this analysis was to seek evidence for or against the existence of an *S*-wave pion-nucleon resonance with $I=\frac{1}{2}$, a resonance suggested by our original analysis² of the scattering. Despite earlier statements³⁰ we have found

²⁹ This point has been made by Watson *et al.* (reference 7) and, in more detail, by M. J. Moravcsik, Phys. Rev. **104**, 1451 (1956).

³⁰ J. Enoch and R. G. Sachs, Bull. Am. Phys. Soc. Ser. II, **1**, 168 (1956). The analysis reported here had been based on the assumption that only *S*- and *P*-wave pions were important. It

no supporting evidence for the resonance. That may only mean that excitation of the resonance state occurs with a small amplitude. On the other hand, nonlinear coupling of the *S* waves could account for the scattering³¹ without recourse to a resonance so there seems to be little reason to invoke the notion of a resonance at the present time.

turns out that the *D* and higher waves contribute a large isotropic term to the cross section which eliminates the need for the *S*-wave resonance.

³¹ Drell, Friedmann, and Zachariasen, Phys. Rev. **104**, 236 (1956).

Mesonic Atoms: Radiative Yields of the π -Meson *L* Series*

M. B. STEARNS, M. STEARNS,† AND L. LEIPUNER‡
Carnegie Institute of Technology, Pittsburgh, Pennsylvania
(Received July 3, 1957)

The total radiative yields of the *L* series from π -mesonic atoms have been measured for most of the elements ${}_{5}\text{B}$ through ${}_{33}\text{As}$. The yield curve has a broad maximum of $\sim 70\%$ in the region $12 \lesssim Z \lesssim 16$ and decreases at both higher and lower *Z* values. This decrease is presumably due to competition from direct nuclear absorption at the higher *Z*'s and to nonradiative processes at the lower *Z*'s. The yields are fairly constant for $25 \lesssim Z \lesssim 30$, suggesting a possible magic number effect at $Z=28$. The rapid decrease in yield with decreasing *Z* cannot be attributed to competition between the simple Auger effect and radiative transitions. The simple Auger transition probabilities are about 40 times smaller than the observed values. More complex nonradiative processes are probably involved, such as those proposed by Day and Morrison.

THE radiative yields of the π -*L* series have been studied by the Carnegie Tech¹ and Rochester² groups. In this paper we report on more recent measurements of these yields. The experimental setup and techniques used are similar to those described in the preceding articles^{3,4} on mesonic x-rays. The corrections to the raw data are similar to those discussed in II,⁴ and they were made in an analogous manner.

The π -*L* mesonic x-ray yields were measured for most of the elements between ${}_{5}\text{B}$ and ${}_{33}\text{As}$ inclusive. These elements and their π - L_{α} transition energies are listed in Table I, columns 1 and 2. A $\frac{1}{16}$ -in. thick NaI crystal was used as the x-ray detector for the elements B through F. A $\frac{1}{2}$ -in. NaI crystal was used for elements F through Si and a 2-in. crystal for Al and all higher *Z* elements. In addition, a 3-in. diameter \times 3-in. thick NaI crystal, stopped down to $\frac{1}{4}$ -in. diameter by a lead collimator, was used for measuring the yields of silicon and higher *Z* elements. Each element was run at least

twice. The meson targets, up to and including titanium, were identical to those used in the μ -meson yield work.⁴ The target material was packed uniformly inside of a thin hollow Lucite cylinder, 1 in. thick and $2\frac{3}{4}$ in. in

TABLE I. Energies and yields of the π -*L* series.

Element	L_{α} energy	Absolute <i>L</i> yield per stopped meson	Ratio of higher transitions to total yield
${}_{5}\text{B}$	12.7	<0.06	
${}_{6}\text{C}$	18.4	0.11 ± 0.015	
${}_{7}\text{N}$	25.1	0.18 ± 0.02	0.28
${}_{8}\text{O}$	32.8	0.25 ± 0.02	0.27
${}_{9}\text{F}$	41.6	0.46 ± 0.05	0.21
${}_{11}\text{Na}$	62.3	0.66 ± 0.04	0.20
${}_{12}\text{Mg}$	74.2	0.67 ± 0.04	0.16
${}_{13}\text{Al}$	87.2	0.70 ± 0.05	0.17
${}_{14}\text{Si}$	101.2	0.69 ± 0.05	0.17
${}_{15}\text{P}$	116.3	0.65 ± 0.04	0.22
${}_{16}\text{S}$	132.4	0.68 ± 0.04	0.27
${}_{17}\text{Cl}$	149.6	0.61 ± 0.04	0.26
${}_{19}\text{K}$	187.1	0.62 ± 0.04	0.21
${}_{20}\text{Ca}$	207.5	0.60 ± 0.04	0.22
${}_{22}\text{Ti}$	251	0.52 ± 0.05	0.25
${}_{24}\text{Cr}$	299	0.38 ± 0.04	0.31
${}_{25}\text{Mn}$	325	0.34 ± 0.06	
${}_{26}\text{Fe}$	352	0.39 ± 0.04	0.27
${}_{27}\text{Co}$	376	0.31 ± 0.06	0.20
${}_{28}\text{Ni}$	405	0.36 ± 0.04	0.23
${}_{29}\text{Cu}$	435	0.40 ± 0.06	
${}_{30}\text{Zn}$	465	0.39 ± 0.05	0.18
${}_{33}\text{As}$	~ 560	<0.19	

* Supported by the U. S. Atomic Energy Commission.

† Present address: General Atomic, San Diego, California.

‡ Now at Brookhaven National Laboratory, Upton, New York.

¹ Stearns, DeBenedetti, Stearns, and Leipuner, Phys. Rev. **93**, 1123 (1954).

² Camac, Halbert, and Platt, Phys. Rev. **99**, 905 (1955).

³ M. Stearns and M. B. Stearns, Phys. Rev. **103**, 1534 (1956), referred to hereafter as I.

⁴ M. B. Stearns and M. Stearns, Phys. Rev. **105**, 1573 (1957), referred to hereafter as II.

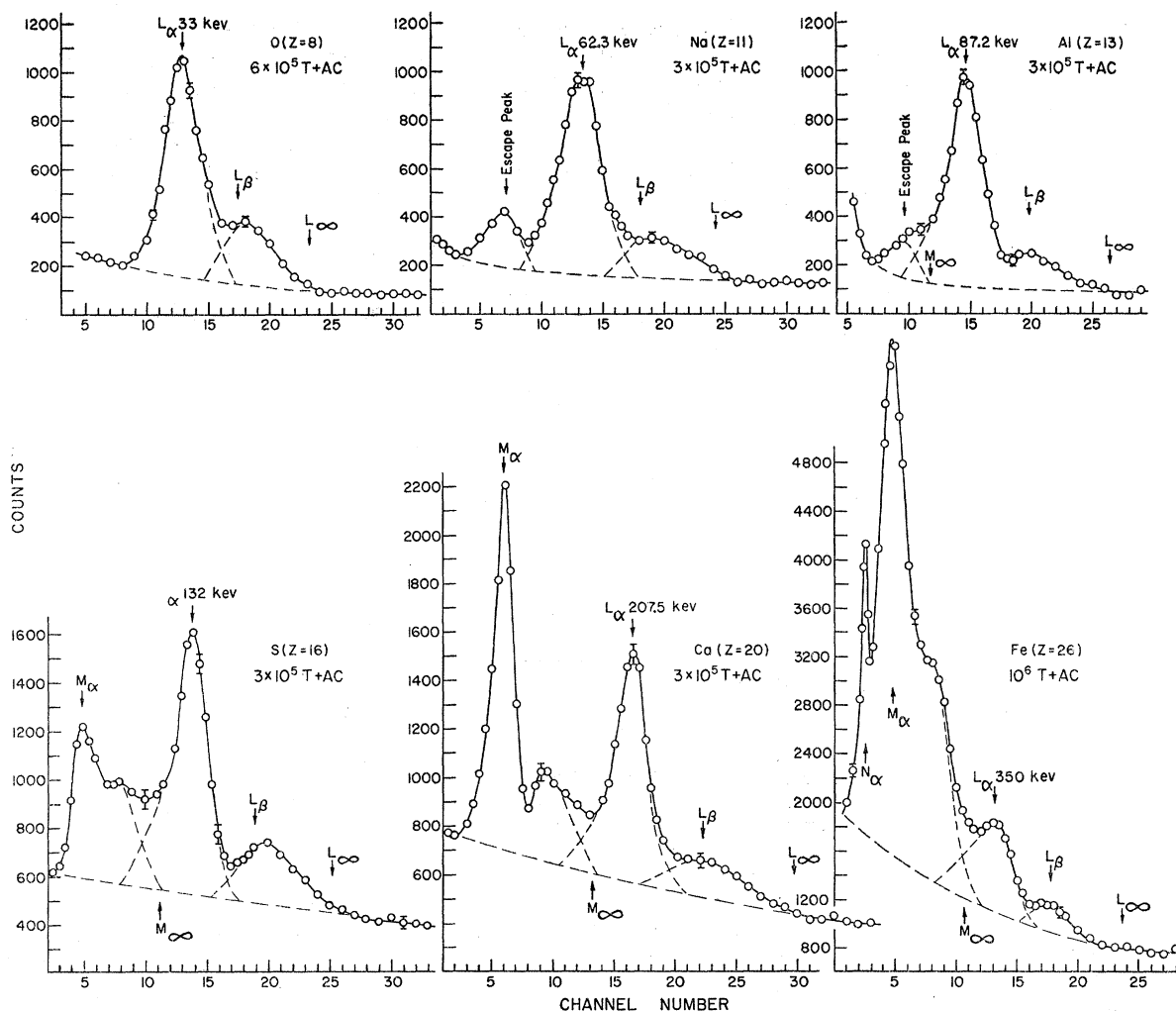


FIG. 1. Typical π -L spectra. In addition to the main L_{α} line there is a high-energy bump contributed by the sum of the higher transitions, L_{β} to L_{∞} . M lines and N lines become increasingly prominent with increasing Z .

diameter, and the thickness in g/cm^2 of each sample was adjusted to be the same and equal to that of water. For titanium and materials of higher Z , the targets were similar in construction but $\frac{1}{2}$ in. thick. Each sample was adjusted to have a surface density of $2.9 g/cm^2$. The relative yields from the two sets of targets were matched at titanium, which was common to both sets.

Typical examples of some of the π -L lines are shown in Fig. 1. These were obtained, as before, by having a 24 channel pulse-height selector scan three or more overlapping energy intervals. This was essential for the proper determination of background since adjacent M lines and higher L lines ($4d \rightarrow 2p$, $5d \rightarrow 2p$, etc.) are not completely resolved. The curves of Fig. 1 are these composite curves. The outstanding features are the main peak due to the $3d \rightarrow 2p$ transition and the high-energy bump, contributed by the sum of the higher transitions. Since $L_{\beta} \approx 1.35L_{\alpha}$, the sum of the higher

transitions and the main peak are more clearly resolved than in the analogous K spectra,⁵ where $K_{\beta} \approx 1.18K_{\alpha}$. M lines are plainly visible in the sulfur yield and become increasingly prominent with increasing Z . Their presence, particularly for $Z > 22$, makes it difficult to obtain accurate L yields. (Not only are the L yields decreasing in this region, but the M lines, because of their lower energy, have a greater detection efficiency.) In order to determine the true background it was necessary to scan the spectrum over the entire region of the M lines and, in some cases, N lines as well. The example of iron, in Fig. 1, illustrates this point. The π - $C(K)$ contamination, originating from mesons stopping in the third counter of the meson telescope, is small in the case of L yields since these yields are large in the region where the correction is important (~ 90 kev). For the Al(L), which overlaps the $C(K)$ line, this correction is about 3%.

⁵ M. Stearns and M. B. Stearns, Phys. Rev. **107**, 1709 (1957).

Table I gives the energies of the L_α lines, the total L -radiative yields per stopped meson, and the ratio of the sum of higher transitions to the total radiative yield. The energies of the L_α lines are calculated values. They were computed from the Klein-Gordon equation, assuming a point charge potential, and corrected for vacuum polarization. Possible additional corrections, discussed in I, have been neglected. The absolute L yields were obtained by measuring the relative L yields as a function of Z and, in a separate experiment, by determining the absolute L yield of aluminum. This is described in the next section. As in the case of K yields,⁵ we define the absolute L yield as the total number of L x-rays emitted per meson stopped in the target. This is the quantity measured experimentally. It is not necessarily equivalent to the total L radiation emitted per mesonic atom. The errors listed in Table I include, in addition to the error arising from the absolute yield determination, uncertainties in the detection efficiency corrections and in the subtraction of backgrounds. The higher transitions constitute about 20–30% of the total yield and are essentially independent of Z . This is similar to the behavior of the higher transitions of the $\pi-K$, $\mu-K$, and $\mu-L$ series.

As in the previous yield determinations, a LiF target was used in the measurement of the fluorine yield. Again no correction was made for the absorption of π mesons by the lithium in the compound. If mesons are captured by the constituent elements of a compound in proportion to Z , as predicted by Fermi and Teller, the measured fluorine yield should be multiplied by the factor $\frac{1}{3}$. To do so, however, would give fluorine an anomalously high yield, putting it far above the curve defined by its neighbors. We have assumed, therefore, that the Li in LiF is ineffectual in absorbing mesons.

Figure 2 is a plot of the total $\pi-L$ radiative yields vs Z . The solid curve is an attempt to fit the experimental points with the function, $\text{const} \times aZ^4 / (c + aZ^4 + bZ^8)$, suggested by competition between radiative transitions (aZ^4), Auger transitions (c), and nuclear capture (bZ^8). The value of a , the L_α radiative transition probability for hydrogen, is readily calculated and is equal to $1.77 \times 10^{10} \text{ sec}^{-1}$. The values of c and b , obtained from fitting the solid curve in Fig. 2, are $c = 1.8 \times 10^{14} \text{ sec}^{-1}$ and $b = 7.1 \times 10^4 \text{ sec}^{-1}$.

The value of c thus derived is about 40 times larger than the theoretical value calculated from the formulas of deBorde.⁶ As discussed in II, this discrepancy cannot be explained by any assumptions involving an isolated mesonic atom. It was shown there that no choice of initial meson capture distribution or subsequent cascade process could produce agreement with experiment. In a recent communication, Day and Morrison⁷ have suggested two additional processes to resolve this discrepancy. Each involves the interaction of a moving

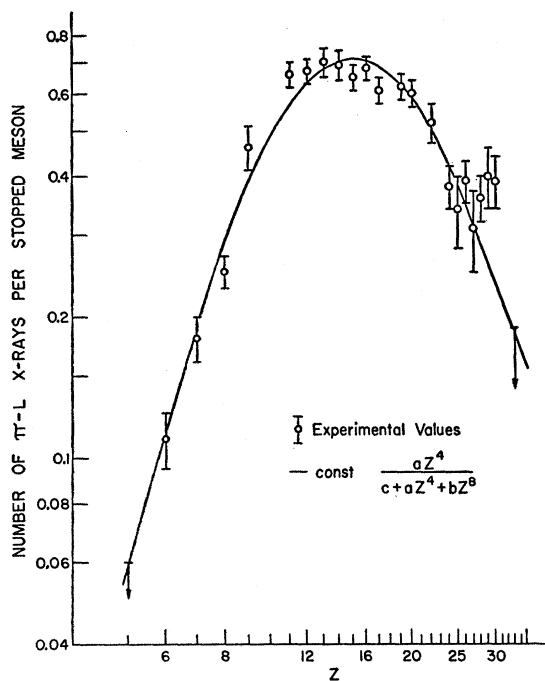


FIG. 2. Relative yields of $\pi-L$ x-rays per stopped meson vs Z . The absolute yields are given in Table I. The formula for the solid curve is suggested by competition between radiative, Auger and nuclear absorption processes.

excited mesonic atom with the normal atoms in condensed matter. In the first process the mesonic atom scatters from a neighboring atom; the meson drops to a lower level, the excess energy being taken off by an electron of the stationary atom. This they call Auger scattering. The second process, called Auger exchange, is similar to the first except that in this case the meson is captured in a lower orbit about the stationary atom. Day and Morrison estimate, for example, that the transition probability for the collisional de-excitation of a μ -mesonic atom from the $2p$ to $1s$ state in a target of lithium metal is roughly 100 times greater than that of the internal Auger effect. This would give good qualitative agreement with experiment.

The eighth power of Z in the nuclear absorption probability is roughly what one would anticipate. Simple theoretical considerations indicate that the nuclear absorption rate might be expected to go as Z^{2l+4} , or Z^8 for d states. Within the admittedly wide limits of the experimental data this, indeed, happens.

The constancy of the yields between $Z=25$ and 30 is tentatively ascribed to a magic-number effect at $Z=28$. This behavior is also observed in the $\pi-K$ series near $Z=8$. Such possible magic-number effects have been mentioned in a paper by Messiah and Marshak.⁸

The $\pi-L$ yields of Camac, Halbert, and Platt² are

⁶ A. H. deBorde, Proc. Phys. Soc. (London) **67**, 57 (1954).

⁷ T. B. Day and P. Morrison, Phys. Rev. **107**, 912 (1957).

⁸ A. M. L. Messiah and R. E. Marshak, Phys. Rev. **88**, 678 (1952).

in general agreement with the yields given in Table I for $Z \leq 16$. However, for larger Z the two sets of data show increasing disagreement. The origin of this discrepancy is very likely due to the different methods used in evaluating the detection efficiency of the NaI crystals. Camac *et al.* calculated their counter efficiency using tables of the total γ -ray absorption coefficient in NaI. This is a difficult and dubious way of obtaining the true crystal efficiency. Edge effects, as well as exactly what value to use for the absorption coefficient, can make the results ambiguous. (See, for example, the work of Rietjens *et al.*⁹) For this reason we feel that the data of Camac *et al.* are not reliable for $Z > 16$. To circumvent this difficulty we have measured the crystal detection efficiency experimentally (for the 2-in. NaI crystal used in this region). These measurements have been described in II.

ABSOLUTE YIELD DETERMINATION

Aluminum L x-rays were used to determine the absolute x-ray yield per stopped meson. This choice was based on the following considerations. The π -Al(L) yield is large and this facilitated the performance of many auxiliary experiments in a reasonable time. Moreover, aluminum is easy to fabricate into the different geometries used in these tests. The energy, 87 kev, is sufficiently high so that absorption corrections in the anticoincidence counter and the aluminum window of the NaI detector are small. On the other hand, the energy is low enough so that the x-rays are completely absorbed by the $\frac{1}{2}$ -in. NaI crystal detector. Moreover, radioactive sources of about this energy are easily obtained and these can be used to study the effect of scattering and self-absorption in the aluminum target. The energy is also convenient for cross-comparisons with μ - K , μ - L , and π - K yields and hence for establishing the absolute yields of these series. Finally, the π -Al(M) yield is still sufficiently small so that background corrections from this source is negligible.

The π -Al(L) line was also used to investigate the mesonic x-ray yield dependence on cyclotron beam strength. It was found that the yield decreased when the cyclotron was run at high intensities. This was not surprising since inefficiencies in the electronics were expected at sufficiently high counting rates. However, when the beam level was reduced below one-half full beam intensity the yield became independent of beam intensity. Therefore all π -meson yield and energy measurements were taken with constant and reduced beam to eliminate this effect.

In order to determine the correct absolute Al(L) yield, it is necessary to know (1) the number of mesonic atoms formed in the aluminum target, and (2) the probability of detection of an Al(L) x-ray. Unfor-

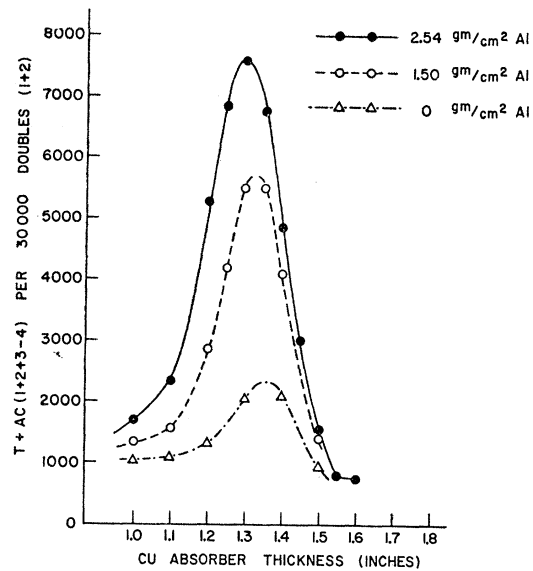


Fig. 3. Differential range curves with different thicknesses of aluminum target. In addition to the variable copper absorber thickness shown on the graph, there was always a fixed 1-in. slab of beryllium and three telescope counters in the beam. The peak with 0 gm/cm² Al is due largely to mesons stopping in the stilbene of counter 3. Because O and Fe have smaller L yields they have been plotted for a greater number of monitor counts (T+AC).

tunately, the number of mesonic atoms formed in the target material cannot be measured directly with the present technique. What is actually measured is the number of mesons *stopped* in the target. These two quantities are not, in general, equivalent. As we observed earlier, some π mesons may be absorbed directly from the continuum without the intermediate formation of a mesonic atom. It is difficult to estimate their number since little is known about the interaction of very slow π mesons with matter. We have, therefore, for convenience defined the absolute yield as the number of x-rays emitted per stopped meson. It should be borne in mind, however, that this quantity is strictly only a *lower* limit to the real absolute yield. For this reason only the shape of the yield *vs* Z curve (Fig. 2) should properly be compared with theory. Actually, this is the most significant feature, since changing the scale of absolute values on the log-log plot translates the curve up or down but does not alter the shape. The relative strengths of Auger transitions, radiative transitions, and nuclear capture are hardly modified. Some authors¹⁰ have sought to make a direct comparison of calculated radiative yields of specific isolated mesonic atoms with experiments. We do not feel that this is advisable at this time.

The number of mesons stopped in the target was determined by taking differential range curves with different thicknesses of target, leaving the rest of the geometry undisturbed. Figure 3 shows differential

⁹ Rietjens, Arkenbout, Walters, and Kluiver, *Physica* 21, 110 (1955).

¹⁰ For example, M. Demeur, *Nuclear Physics* (North Holland Publishing Company, Amsterdam, 1956), Vol. 1, p. 516.

range curves for 2.54 g/cm², 1.50 g/cm², and 0 g/cm² of aluminum. The ordinate is the meson telescope counting rate, triples plus anticoincidence (T+AC), (1+2+3-4) per 30 000 doubles (1+2) used as a monitor. The abscissa is the copper absorber thickness. In addition to the variable copper thickness there was always a 1-in. thick slab of beryllium in front of counter 3. The peak with 0 g/cm Al is due largely to mesons stopping in the stilbene of counter 3. The range curves were analyzed in several ways in order to estimate the number of mesons lost by nuclear absorption and scattering in flight. However, in practice it was found that the number of stopped mesons could be determined sufficiently accurately by simply taking the difference in the T+AC counting rate with target and without. This procedure introduces a small error since some mesons which miss the AC counter when the target is absent will, in fact, be stopped in the target when it is present. However, in view of the close geometry and the relatively large size of the AC counter, this effect is small.

The probability of detection of a mesonic x-ray depends on the effective size of the target, the solid angle subtended by the detector, the efficiency of the detector, and the absorption and scattering in the intervening material. As described in II, the effective area of the aluminum target was only slightly larger than the area of counter 3 of the meson telescope. This was determined by measuring the Al(*L*) x-ray yield as a function of target area, the target thickness remaining constant. It was found that the Al(*L*) yield increased with increasing area up to a size slightly larger than counter 3. For areas larger than this the yield remained sensibly constant. This result, in addition to defining the effective target area, indicates that the mesons were not scattered appreciably in the moderating material.

The over-all detection efficiency was determined by numerical calculation as follows. The aluminum target was divided into 48 equal volumes (the effective cross-

sectional area being subdivided into 16 equal areas and the thickness into 3 equal slabs). The NaI detector ($\frac{1}{2}$ -in. thick crystal) was also sectioned into 9 equal areas. The solid angle subtended by each segment of the detector as seen from the center of each of the 48 volumes of the target was calculated. In each case this was corrected for the attenuation that an 87-keV x-ray (Al-*L_α*) would undergo in traversing the anticoincidence counter and the aluminum window of the NaI detector. The detection efficiency of the NaI crystal for an 87-keV x-ray can be taken to be 100%. A suitable average was then made over all the x-ray trajectories and solid angles to obtain the detection efficiency. The correction for scattering and absorption in the aluminum target itself was too difficult to estimate theoretically and was obtained experimentally with artificial radioactive sources. This measurement is discussed in Sec. II-D of reference 4. The over-all detection efficiency determined in this manner was 5.8%.

The experimental *L* yields presented here can be easily understood on a qualitative basis in terms of competition between radiative, capture, and simple Auger processes. Quantitative agreement with theory, however, is more difficult to achieve, particularly for *Z* < 11. More complex processes, such as those proposed by Day and Morrison, must be operative in this region. Since these depend on the condensed nature of the target material, it would be useful to measure the radiative yield of, say, nitrogen or oxygen (or air) as a function of gas pressure. As the authors suggest, this would test their assumptions directly.

ACKNOWLEDGMENTS

It is a pleasure to acknowledge the collaboration of Professor S. DeBenedetti in the earlier phases of this experiment. We are most grateful to Dr. Day and Professor Morrison for the communication of their results prior to publication.